Experimental Gerontology 147 (2021) 111267

Contents lists available at ScienceDirect

Experimental Gerontology

journal homepage: www.elsevier.com/locate/expgero

Estradiol deficiency and skeletal muscle apoptosis: Possible contribution of microRNAs

Sira Karvinen [a,*], Hanna-Kaarina Juppi [a], Gengyun Le [b], Christine A. Cabelka [b,c], Tara L. Mader [b,d], Dawn A. Lowe [b], Eija K. Laakkonen [a]

[a] Gerontology Research Center, Faculty of Sport and Health Sciences, University of Jyväskylä, Jyväskylä, Finland
[b] Divisions of Rehabilitation Science and Physical Therapy, Department of Rehabilitation Medicine, Medical School, University of Minnesota, Minneapolis, MN, USA
[c] Department of Physical Therapy, The College of St. Scholastica, Duluth, MN, USA
[d] Health, Physical Education, and Exercise Science Department, Division of Professional Studies, Augsburg University, Minneapolis, MN, USA

ARTICLE INFO

Section Editor: Werner Zwerschke

Keywords:
Menopause
Ovariectomy
Muscle mass
Caspase
Cytochrome C

ABSTRACT

Background: Menopause leads to estradiol (E_2) deficiency that is associated with decreases in muscle mass and strength. Here we studied the effect of E_2 deficiency on microRNA (miR) signaling that targets apoptotic pathways.

Methods: C57BL6 mice were divided into control (normal estrous cycle, $n = 8$), OVX (E_2 deficiency, $n = 7$) and OVX + E_2 groups (E_2-pellet, $n = 4$). Six weeks following the OVX surgery, mice were sacrificed and RNA isolated from gastrocnemius muscles. miR-profiles were studied with Next-Generation Sequencing (NGS) and candidate miRs verified using qPCR. The target proteins of the miRs were found using in silico analysis and measured at mRNA (qPCR) and protein levels (Western blot).

Results: Of the apoptosis-linked miRs present, eleven (miRs-92a-3p, 122-5p, 133a-3p, 214-3p, 337-3p, 381-3p, 483-3p, 483-5p, 491-5p, 501-5p and 652-3p) indicated differential expression between OVX and OVX + E_2 mice in NGS analysis. In qPCR verification, muscle from OVX mice had lower expression of all eleven miRs compared with OVX + E_2 ($p < 0.050$). Accordingly, OVX had higher expression of cytochrome C and caspases 6 and 9 compared with OVX + E_2 at the mRNA level ($p < 0.050$). At the protein level, OVX also had lower anti-apoptotic BCL-W and greater pro-apoptotic cytochrome C and active caspase 9 compared with OVX + E_2 ($p < 0.050$).

Conclusion: E_2 deficiency downregulated several miRs related to apoptotic pathways thus releasing their targets from miR-mediated suppression, which may lead to increased apoptosis and contribute to reduced skeletal muscle mass.

1. Introduction

Levels of estrogens decline during menopause and this is associated with decreases in muscle mass and strength (Juppi et al., 2020; Maltais et al., 2009; Bondarev et al., 2020). We and others have shown that estrogen replacement therapy partially offsets these unfavorable changes in skeletal muscle mass and function in postmenopausal women (Sipila et al., 2001; Taaffe et al., 2005; Ronkainen et al., 2009; Greising et al., 2009). Similarly, estrogen deficiency in animal models has been shown to mediate decrements in muscle strength (Greising et al., 2009; Moran et al., 2006; Collins et al., 2019a) and treatment with estradiol (E_2) reverses or prevents strength loss (Greising et al., 2009; Moran et al., 2007; Schneider et al., 2004). Furthermore, it was found that ovarian hormones have a critical role in the regrowth of atrophied skeletal muscle and in the regulation of muscle stem cell function and regeneration in female mice (Collins et al., 2019a; Sitnick et al., 2006; McClung et al., 2006; Moore et al., 2019). Yet the mechanistic role of estrogens in the loss of muscle mass has not been established.

Abbreviations: AIF, Apoptosis inducing factor; BCL2, B-cell lymphoma-2 regulator protein; BCL-XL, B-cell lymphoma-extra-large regulator protein; BCL-W, B-cell lymphoma-like protein 2; CASP, Caspase; cytC, Cytochrome C; E_2, Estradiol; FasL, Fas ligand; GAPDH, Glyceraldehyde 3-phosphate dehydrogenase; HSP, Heat shock protein; miR, microRNA; NGS, Next-generation sequencing; OVX, Ovariectomy.

* Corresponding author at: P.O. Box 35 (VIV148), FI-40014 University of Jyväskylä, Finland.
E-mail address: sira.m.karvinen@jyu.fi (S. Karvinen).

https://doi.org/10.1016/j.exger.2021.111267
Received 28 August 2020; Received in revised form 25 January 2021; Accepted 27 January 2021
Available online 4 February 2021

The degenerative loss of skeletal muscle mass, quality, and strength associated with ageing is termed sarcopenia (Doherty, 2003). Both muscle mass and fiber number decrease significantly with ageing (Brown et al., 1992; Evans, 1995). Programmed cell death termed apoptosis is a highly coordinated signaling cascade leading to elimination of cells. Apoptosis is a key mechanism in normal development of multicellular organisms and is involved in cell turnover and ontogenesis (Steller, 1995). Apoptosis has been proposed to be a key signaling route also in skeletal muscle homeostasis, including muscle ageing and sarcopenia (Dirks and Leeuwenburgh, 2002; Marzetti and Leeuwenburgh, 2006).

There are two major apoptotic signaling pathways: the extrinsic (death receptor) and intrinsic (mitochondrial) apoptotic pathways (Fig. 1) (Hassan et al., 2014). The extrinsic pathway of apoptosis is mediated via the tumor necrosis factor (TNF) family receptors, such as Fas ligand (FasL), initiated by external stimuli that leads to activation of caspases (CASP) 8 and 10 (Hassan et al., 2014; Locksley et al., 2001). Consecutively, the intrinsic apoptotic pathway can be triggered by a variety of intracellular stimuli, such as oxidative stress and DNA damage (Wu and Bratton, 2013). In the intrinsic pathway, apoptosis is induced via release of cytochrome C (cytC) from mitochondria into the cytosol leading to assembly of a multiprotein complex termed apoptosome (Green and Kroemer, 2004). Apoptosome is composed of procaspase 9, apoptotic protease activating factor 1 and cytC. In addition, several B cell lymphoma-2 (BCL2) family members including BCL2, BCL-W and B-cell lymphoma-extra-large (BCL-XL) act as anti-apoptotic proteins by controlling the release of cytC to the cytosol and regulating mitochondrial membrane permeabilization (Green and Kroemer, 2004). Downstream, both intrinsic and extrinsic apoptotic pathways are mediated through CASPs, a family of proteases that provide critical links in cell signaling networks and cell death (McIlwain et al., 2015). In addition, apoptosis can be initiated independent of CASPs via apoptosis inducing factor (AIF) that triggers DNA fragmentation (Joza et al., 2009). Upstream, tumor protein p53 serves as a regulator that can modulate key control points in both the extrinsic and intrinsic apoptotic pathways (Fridman and Lowe, 2003).

Estrogen has been shown to protect against apoptosis in non-skeletal muscle tissues as well as in muscle progenitor cells (Hou et al., 2010; Ruan et al., 2014; La Colla et al., 2013). Furthermore, it has been suggested that estrogens possess a protective role against cellular damage in heart muscle by increasing the expression of the protective heat shock proteins (HSPs) (Knowlton and Korzick, 2014). In muscle biopsies from human twins, E_2 deficiency has been associated with cell death, apoptosis, and cell survival with E_2 being the predicted upstream regulator of these processes (Laakkonen et al., 2017). However, the possible mechanistic role of E_2 deficiency in skeletal muscle apoptosis contributing to sarcopenia has not been elucidated.

One possible route through which E_2 may coordinate skeletal muscle apoptosis involves microRNAs (miRs). miRs are a small non-coding RNA molecules that function in post-transcriptional regulation of gene expression either by targeting mRNAs for degradation or inhibiting transcription initiation (Krol et al., 2010). miRs have been shown to alter gene expression in skeletal muscle in response to various external stimuli such as exercise (Krol et al., 2010; Sapp et al., 2017) and estrogen

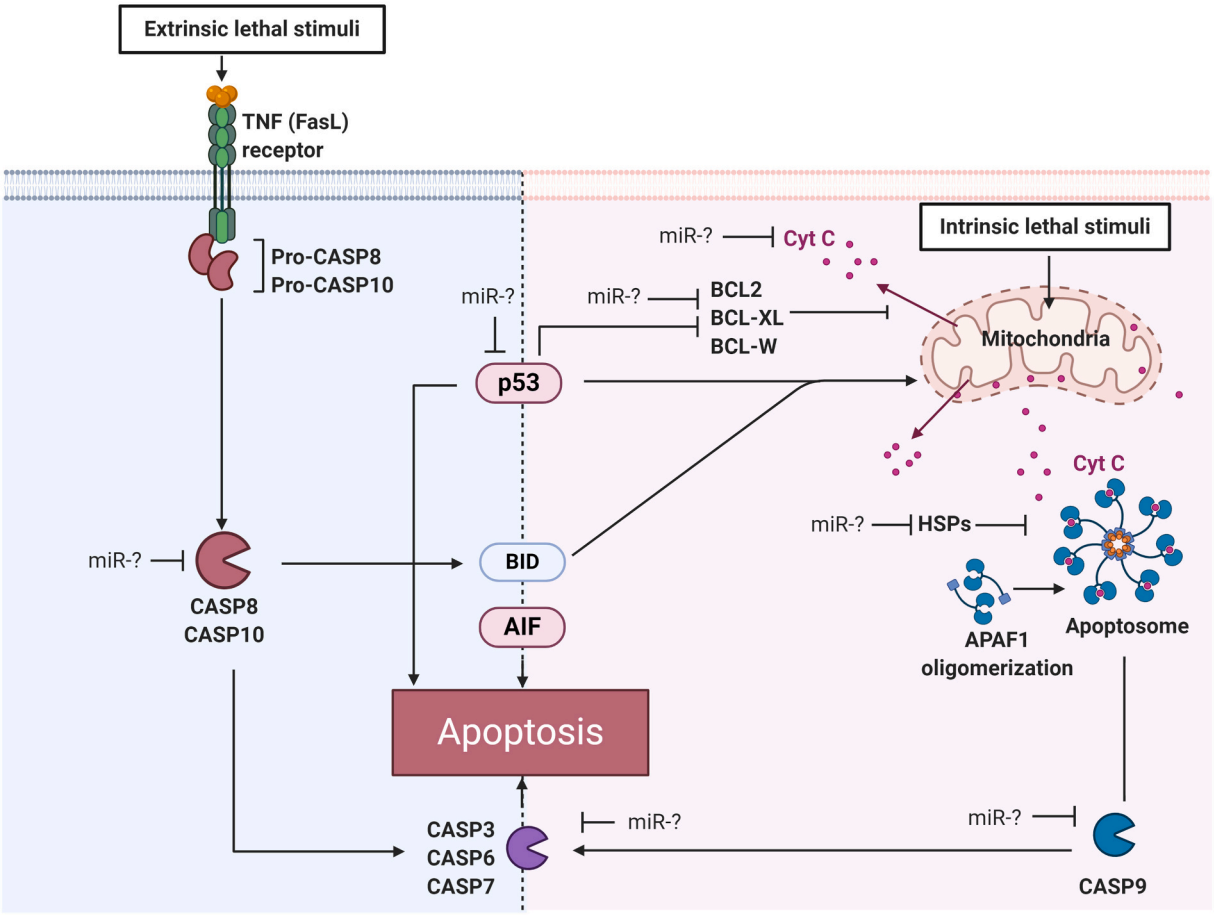

Fig. 1. Schematic of apoptotic pathways. Key proteins of extrinsic and intrinsic apoptotic pathways that are possibly regulated by miRs are shown. TNF = tumor necrosis factor, FasL = Fas ligand, CASP = caspase, BCL2 = B-cell lymphoma-2 regulator protein, BCL-XL = B-cell lymphoma-extra-large regulator protein, BCL-W=B-cell lymphoma-like protein 2, BID=Protein of the B-cell lymphoma-2 regulator family, AIF = Apoptosis inducing factor, p53 = tumor protein, cytC = cytochrome C, HSP=Heat shock protein, miR = microRNA. Figure was created in BioRender.com.

status (Olivieri et al., 2014). To date several miRs have been identified to regulate apoptosis at many steps leading to programmed cell death (Su et al., 2015a). In the apoptosis field, the vast majority of miR studies have concentrated on cancer biology. These studies revealed divergent roles of miRs along the apoptosis pathways, mainly by acting as tumor suppressors by inhibiting the function of key proteins inducing cell death (Dar et al., 2013; Bai et al., 2009; Sun et al., 2017).

Here we studied the effect of E_2 deficiency on miR signaling coordinating the initiation of skeletal muscle apoptosis to determine if miRs associate with E_2 and activation of apoptotic signaling cascades in skeletal muscle. In the present study we utilized C57BL6 mice with three study groups; control (normal estrous cycle), OVX (E_2 deficiency due to ovariectomy) and OVX + E_2 (E_2 supplemented by pellet). The aim of our study was to determine the link between E_2 and the initiation of skeletal muscle apoptosis. Our hypothesis was that E_2 deficiency is associated with lower expression of apoptosis-linked miRs, which leads to increased expression of proteins along apoptotic pathways.

2. Methods

2.1. Animal experiment

Female C57BL/6J mice aged 3–4 months were obtained from The Jackson Laboratory (Bar Harbor, ME, USA). Mice were housed in groups of four to five and had phytoestrogen-free rodent feed (Harlan-Teklad no. 2019; Indianapolis, IN, USA) and water ad libitum. The housing room was maintained on a 14:10 h light:dark cycle with controlled temperature and humidity.

Mice were randomly divided into three groups: control ($n = 8$), OVX ($n = 7$) and OVX + E_2 ($n = 4$). At 4–6 month of age surgical procedures were conducted as described previously (Moran et al., 2007) with the exception that 2 h prior to surgery, mice were given a subcutaneous injection of slow-release buprenorphine (2 mg/kg) in the hindlimb area. Briefly, mice were then anesthetized with isoflurane and ovariectomy was performed under aseptic conditions through two small dorsal incisions between the iliac crest and the lower ribs. In OVX + E_2 mice, a slow-release 17β-estradiol-containing pellet (E_2 pellet) was placed subcutaneously in the neck area immediately following OVX while still under anesthesia. The E_2 pellets used in this study had 0.18 mg of 17β-estradiol released over a 60-day period (Innovative Research of America, Sarasota, FL, USA) resulting in physiological serum E_2 levels (Moran et al., 2007; Le et al., 2018). Half of the mice (n = 4) in the control group underwent the same surgery as the OVX mice without removal of the ovaries (~sham surgery), while four mice had no surgery. For all variables measured, there were no differences between sham mice and mice that had no surgery ($p > 0.05$) and therefore, data for these two groups of mice were collapsed to constitute the control group. Mice were sacrificed 5–8 weeks later and at this time successful OVX and E_2 treatment were verified by vaginal cytology or uterine mass. Body mass at the time of sacrifice was (mean ± SD); control = 23.9 ± 2.0 g, OVX = 26.5 ± 2.4 g, and OVX + E_2 = 23.8 ± 1.4 g.

Mice were sacrificed by an overdose of pentobarbital sodium (200 mg/ kg) and skeletal muscles from the hind limbs were harvested, snap frozen in liquid nitrogen, and stored at −80 °C.

2.2. Skeletal muscle sample processing

2.2.1. miR and mRNA isolation

miRs and mRNA were isolated from frozen gastrocnemius muscles by miRNeasy Mini Kit (Qiagen, cat. no. 217004) according to manufacturer's instructions. 40–50 mg of the muscle sample was used for the procedure. Briefly, frozen muscle sample was homogenized in 700 μl of Qiazol lysis reagent in TissueLyser with magnetic beads. Homogenate was incubated at room temperature (RT) for 5 min and 140 μl chloroform was added. Tubes were shaken 15 s, incubated at RT for 3 min and centrifuged for 15 min at 12000 xg at 4 °C. The upper aqueous phase was transferred to a new collection tube and the protocol was followed according to the manufacturer's instructions until RNA was eluted from the column.

2.2.2. Protein isolation

Remaining gastrocnemius muscle samples were homogenized by a TissueLyser with metallic beads in a lysis buffer that contained Tissue extraction Reagent I buffer (TERI, Invitrogen, FNN0071) supplemented with 10 μl/ml of the following protease inhibitors: Halt Protease and Phosphatase Inhibitor Cocktail with EDTA (Pierce 78444) and pepstatin A (Sigma P5318). 15 μl/mg of the lysis buffer mix was used for each muscle sample. Samples were mixed for 30 min in end-over-end rotation at +4 °C. Thereafter, samples were centrifuged for 10 min at 10000 *g* at +4 °C. Total protein of the supernatant was measured using a BCA protein assay (Pierce™ *BCA Protein Assay* Kit #23227).

2.3. miR analysis by NGS

Total RNA samples were prepared for explorative NGS analysis with pooled samples of the studied groups; control(pool), OVX(pool) and OVX + E_2(pool). The control(pool) was comprised of ovary-intact mice (both sham-operated mice and mice that did not undergo any surgery). From each individual sample, 1000 ng of RNA was used for making the pool. Thereafter, pooled samples from the control, OVX and OVX + E_2 groups were diluted according to manufacturer's instructions to 20 ng/μl, of which 5 μl was used for the miR-library (total 100 ng of sample).

For the miR library, QIAseq miRNA Library Kit (Cat no. 331502) with QIAseq miRNA index kit (Cat no 331592) was used. MiR sequencing was performed using the NextSeq 500/550 high Output v2 kit (75 cycles) (FC-404-2005, Illumina) run with NextSeq500 equipment. The raw data was processed using the Secondary QIASeq miRNA Library Kit Data Analysis Software that analyzes the Unique Molecular Index (UMI) counts to calculate changes in the miR expression. For the analysis, control was set as control group with Trimmed mean selected as a normalization method. The differential expression of miRs between OVX(pool) and OVX + E_2(pool) samples were reported as fold change relative to control group. Cut point for target miR selection was set at >100 reads (i.e., at least one group had to have had >100 reads of the target miR).

2.4. In silico analysis of miR target genes

The search for miR target genes on apoptotic pathways was performed using four different miR target databases: TargetScan, Diana, PicTar and miRWalk as well as Ingenuity Pathway Analysis (IPA, version 57662101, Qiagen). Utilizing these four miR databases together with IPA enabled analyses of a more comprehensive atlas of predicted and validated miR targets than by using only a single database.

2.5. miR analysis by qPCR

Expression of the miRs selected from the NGS miR-library based on in silico analysis were confirmed with qPCR using the following primers from Qiagen: miR-92a-3p (MS00005971), miR-122-5p (MS00003416), miR-133a-3p (MS00031423), miR-214-3p (MS00031605), miR-337-3p (MS00011844), miR-381-3p (MS00004116), miR-483-3p (MS00007693), miR-483-5p (MS00012264), miR-491-5p (MS00004326), miR-501-5p (MS00032935) and miR-652-3p (MS00010451). Samples were run as triplicates. qPCR results were analyzed with the ΔΔCt method and are expressed as fold change relative to control samples.

2.6. Gene expression analysis by qPCR

MiRs targeted proteins on the apoptosis pathways were measured by mRNA expression levels using the following primers from Qiagen:

GAPDH (NM_008084), CASP3 (NM_00981), CASP6 (NM_009811), CASP8 (NM_009812), CASP9 (NM_015733), BCL2 (NM_009741), BCL-W (official name: Bcl2l2, NM_007537), BCL-XL (official name: Bcl2l1, NM_009743), cytC (official name: Cycs, NM_007808) and p53 (official name: Trp53, NM_011640). Samples were run as triplicates. qPCR results were analyzed with the ΔΔCt method and are expressed as fold change relative to OVx + E_2 samples.

2.7. Protein expression analysis by Western blotting

The level of several proteins on the apoptotic pathways were quantified using Western blot. Briefly, 30 μg of isolated protein from gastrocnemius muscle was used from each sample. Samples were first heated for 10 min at 95 °C in sample buffer (1:1 in 20:1 Laemmli and 5% β-mercaptoethanol) and run for 35 min in a Stain Free gradient gel (4–20%, BioRad) at 270 V. Proteins were blotted onto nitrocellulose membrane and total protein was visualized after protein transfer. Thereafter, membranes were blocked for 2 h at RT in blocking buffer (Odyssey) and incubated with primary antibody in 1:1 TBS and blocking buffer +4 °C overnight. The following antibodies were used: CASP3 (active) (#9661, 1:1000, Cell Signaling) CASP6 (inactive and active) (ab185645, 1:1000, Abcam), CASP8 (inactive) (ab25901, 1:1000, Abcam), CASP9 (active) (#9509, Cell Signaling, 1:1000), CASP9 (inactive) (ab202068, 1:2000, Abcam), BCL2 (ab692, 1:500, Abcam), BCL-W (#2724, 1:1000, Cell Signaling), BCL-XL (ab32370, 1:1000, Abcam), cytC (ab90529, 1:2000, Abcam), p53 (official name: Trp53, ab26, 1:500, Abcam), AIF (Sc-13,116, 1:200, Santa Cruz), CRYAB (official name: Hspb5, #45844S, 1:1000, Cell Signaling), HSP27 (official name: HSPB1, CPTC-HSPB1-1, 1:500, Hybridoma Bank) and HSP60 (official name: Hspd1, #4870, 1:500, Cell Signaling). Membranes were then washed and incubated with secondary antibody for 1 h at RT (1:1 TBS-T and blocking buffer), washed and visualized. Proteins were quantified using Image Lab software. First, the results were normalized to the average signal of the membrane and thereafter to corresponding total protein amount obtained from the whole membrane blotted from a stain free gel (whole protein lane). Results are expressed as fold change relative to OVx + E_2 samples.

2.8. Statistical analyses

Results are presented as mean and standard error of means (SEM). The normality of variables was assessed using Shapiro-Wilks tests followed by Levene's test for examining the equality of the variances. First, the extreme outliers were excluded from the analysis (>3× interquartile range). When the normality criteria were met, differences between the groups (OVX and OVX + E_2) were examined using Student's *t*-test (Western blot protein expression levels). When the normality criteria were not fulfilled, differences between the groups were examined using Kruskal-Wallis test followed by Mann-Whitney *U* test (qPCR results for miRs) or Mann-Whitney *U* test (mRNA levels). Data analyses were carried out using IBM SPSS Statistics software version 24 (Chicago, IL, US), and the level of significance was set at $p \leq 0.050$.

3. Results

3.1. NGS identification of miRs

NGS analysis was done to first verify the most abundant miRs and second to explore the specific miRs that respond to E_2 in skeletal muscle. The two most abundant miRs in all groups of mice, miR-1a-3p and miR-133a-3p, are muscle specific miRs (Table 1).

3.2. E_2 responsive miRs that target apoptotic pathways

To investigate the possible link between E_2 deficiency and miR-mediated regulation of apoptotic signaling, we focused on apoptosis-linked miRs. In silico analysis with four different databases and IPA showed that eleven miRs identified to be responsive to E_2 (Table 2) have several targets on apoptotic pathways (Table 3). NGS analysis of the E_2 sensitive miRs was run comparing OVX and OVX + E_2 each to the control group and indicated differential expression patterns between OVX and OVX + E_2 mice. These apoptosis-linked, differentially expressed E_2-responsive miRs were used as candidate signaling modulators of apoptosis.

Results of *in slico* analysis were not completely consistent between the databases (Table 3). For example, only miRs-133a-3p and 214-3p were found to target apoptosis-linked proteins in all four of the miR

Table 1
Twenty most abundant miRs according to reads in NGS analysis in muscle from control, OVX and OVX + E2 groups.

Rank	Control		OVX		OVX + E2	
	miR	Reads	miR	Reads	miR	Reads
1	**miR-1a-3p**	21,097,106	**miR-1a-3p**	17,434,920	**miR-1a-3p**	19,618,500
2	**miR-133a-3p**	2,616,739	**miR-133a-3p**	2,469,748	**miR-133a-3p**	3,176,871
3	miR-126a-3p	585,076	miR-126a-3p	727,958	let-7f-5p	738,205
4	let-7f-5p	574,105	let-7f-5p	701,060	miR-126a-3p	586,756
5	miR-143-3p	504,622	miR-16-5p	563,935	miR-16-5p	500,677
6	miR-26a-5p	481,154	miR-26a-5p	522,538	miR-26a-5p	490,611
7	miR-16-5p	443,756	miR-143-3p	518,288	let-7a-5p	476,089
8	let-7a-5p	316,171	let-7a-5p	419,319	miR-143-3p	409,992
9	miR-125b-5p	302,611	miR-125b-5p	349,376	miR-125b-5p	320,767
10	miR-30a-5p	296,285	**miR-206-3p**	328,095	let-7i-5p	300,807
11	**miR-206-3p**	259,993	let-7c-5p	323,725	let-7c-5p	294,044
12	miR-1b-5p	251,335	let-7i-5p	289,413	**miR-206-3p**	288,776
13	let-7i-5p	238,688	miR-30a-5p	254,499	miR-378a-3p	269,323
14	let-7c-5p	233,160	miR-378a-3p	236,223	miR-30a-5p	268,885
15	miR-378a-3p	232,999	miR-1b-5p	231,988	miR-1b-5p	247,180
16	miR-29a-3p	211,195	miR-29a-3p	209,769	miR-29a-3p	206,621
17	miR-26b-5p	164,072	miR-26b-5p	186,750	miR-26b-5p	172,737
18	miR-126a-5p	156,207	let-7b-5p	162,794	let-7b-5p	159,892
19	miR-101a-3p	143,259	miR-126a-5p	158,968	miR-126a-5p	134,825
20	miR-199a/b-3p	127,357	miR-101a-3p	145,617	miR-199a/b-3p	132,129

Muscle specific miRs are bolded.

Table 2
Estradiol-responsive, apoptosis-linked miRs that showed differential expression between muscle from OVX and OVX + E_2 mice (expressed as fold change relative to control).

miR ID	OVX	OVX + E_2
miR-92a-3p	0.99	1.42
miR-122-5p	0.78	2.64
miR-133a-3p	0.85	1.21
miR-214-3p	0.91	1.28
miR-337-3p	0.95	1.63
miR-381-3p	0.80	2.18
miR-483-3p	0.78	2.53
miR-483-5p	1.04	2.11
miR-491-5p	1.37	1.95
miR-501-5p	1.39	0.48
miR-652-3p	1.20	0.94

databases as well as IPA and only miRwalk and IPA found putative apoptosis-linked target proteins for each of the studied miRs. Table 3 shows also experimentally validated associations between miR and its target protein.

3.3. qPCR – expression levels of putative E_2 sensitive miRs

The expression of the potential target miRs found from NGS were confirmed by qPCR (Fig. 2). In Fig. 2, the triangles for control group represent the mice that did not undergo any surgery and black dots represent sham-operated mice. Because data from sham-operated mice and those that had no surgery did not differ ($p \geq 0.072$), these subpopulations were combined to form one control (ovary-intact) group for further statistical analyses. Due to an extreme value that was not detected as a true outlier found in miR-122-5p data in group OVX + E_2 (Fig. 2B), the analysis was run excluding that highest data point. Excluding the one data point did not change the results between the groups (see Supplementary Fig. 1). Kruskal-Wallis test showed significant difference between the groups for each of the eleven miRs ($p \leq 0.044$). Post hoc analyses showed that muscles from OVX mice had lower expression of all eleven of the studied miRs compared with OVX + E_2 ($p \leq 0.017$, Fig. 2). OVX muscles also had lower miRs 122-5p and 214-3p expression compared with control ($p \leq 0.028$, Fig. 2B, D). OVX + E_2 muscles had higher expression of miRs 92a-3p, 133a-3p, 214-3p, 381-3p, 483-3p, 483-5p and 491-5p than controls ($p \leq 0.042$, Fig. 2A, C-D, F-I).

3.4. qPCR – mRNA expression of miR targets

To concentrate on the extremes of systemic E_2 level, we continued the analysis with the group of the lowest systemic E_2 level (OVX) and the constantly high E_2 level (OVX + E_2) to avoid the possible confounding effect of the cyclic nature of systemic E_2 level in the control group. The mRNA expression of predicted miR targets on apoptosis pathways were measured using qPCR (Figs. 3 and 4). OVX muscles had higher expression of CASPs 6 and 9 compared to OVX + E_2 muscles ($p \leq 0.023$; Fig. 3B, D) but not CASP3 or CASP8 ($p = 0.571$, $p = 0.072$, respectively, Fig. 4A, C).

OVX muscles had higher cytC and p53 mRNA expressions compared to OVX + E_2 ($p \leq 0.038$; Fig. 4D-E) whereas no changes were observed in BCL2, BCL-XL or BCL-W.

3.5. Western blot - protein expression of miR targets

The protein levels of key CASPs are presented in Fig. 5. Muscles from mice in the OVX group had a lower inactive CASP8 level ($p = 0.028$, Fig. 5B) and higher active CASP9 compared with OVX + E_2 muscles ($p = 0.046$, Fig. 5F). There were no significant findings in the other CASPs measured ($p \geq 0.140$).

The Western blot results from additional apoptosis-linked proteins are presented in Fig. 6. OVX muscles had lower BCL-W and higher cytC levels compared to OVX + E_2 ($p = 0.010$, $p = 0.023$, respectively; Fig. 6C, F). There were no significant findings in the other proteins studied ($p \geq 0.108$).

The Western blot results from HSPs are presented in Fig. 7. OVX muscles had lower levels of CRYAB and HSP60 and a higher level of HSP27 compared to OVX + E_2 ($p \leq 0.008$; Fig. 7).

4. Discussion

Our results were in line with our hypothesis, that E_2 deficiency was associated with lower expression of apoptosis-linked miRs. Consequently, E_2 deficiency led to higher mRNA expression of pro-apoptotic cytC, p53 and CASPs 6 and 9 and greater protein abundance of cytC and active CASP9. However, we also discovered lower protein abundance of anti-apoptotic BCL-W, CRYAB and HSP60 and greater abundance of HSP27. Our data suggests that E_2 deficiency may play a role in

Table 3
In silico analysis of miR target genes via four miR target databases, IPA and experimentally validated associations between miR and target protein.

miR	TargetScan	Diana	miRwalk	PicTar	IPA	Experimentally shown miR-target associations
miR-92a-3p	FasL	–	CASP3, CASP8, CASP9, HSP60, CytC	–	p53	CASP3, BCL2 (Li et al., 2019)
miR-122-5p	–	–	CASP3, CASP8, BCL-XL, BCL-W, HSP60, CytC	BCL-W	BCL-W	CASP8, BCL2, BCL-XL, p53 (Yin et al., 2011; Zhang et al., 2017)
miR-133a-3p	BCL-XL, BCL-W	BCL-XL	CASP3, CASP8, CASP9, BCL2, BCL-XL, BCL-W, HSP60, CytC	BCL-XL, BCL-W	BCL-XL, BCL-W	CASP3, CASP9, BCL-XL (Chen et al., 2016; Ji et al., 2013)
miR-214-3p	HSP27, Casp2	HSP27	CASP3, CASP6, CASP8, BCL-W	BCL-XL, HSP60	HSP27	BCL-W, HSP70 (Bai et al., 2020; Fan and Wu, 2017)
miR-337-3p	–	–	CASP9, BCL-XL, BCL-W	–	BCL-XL, BCL-W	CASP3, CASP7, BCL2 (Xia et al., 2019; Park et al., 2018)
miR-381-3p	–	–	CASP3, CASP8, CASP9, BCL2, BCL-XL, BCL-W, CytC	–	CASP6	CASP3, CASP8, CASP9, BCL2 (Zhao et al., 2020; Qiao et al., 2019; Shang et al., 2019)
miR-483-3p	–	–	CASP3, CASP6, CASP8, BCL-XL, BCL-W, HSP60, CytC	–	FasL	CASP3, BCL2, p53 (Veronese et al., 2010; Lu et al., 2020)
miR-483-5p	–	–	CASP3, CASP6, CASP8, CASP9, BCL-XL, BCL-W, CytC	–	CASP3, CASP8	CASP3, BCL2 (Wu et al., 2016; Liu et al., 2019)
miR-491-5p	–	–	CASP3, CASP6, CASP8, CytC, FasL, BCL2, BCL-W	–	p53, CRYAB	BCL-XL, p53 (Guo et al., 2012)
miR-501-5p	–	–	CASP3, CASP6, CASP8, CASP9, BCL2, BCL-XL, BCL-W, CytC	–	p53, HSP60, cytC	BCL2 (Sanches et al., 2018)
miR-652-3p	–	–	CASP3, CASP8, CASP9, BCL2, BCL-XL, BCL-W, CytC	–	p53, CASP3, CASP6	CASP3, BCL2 (Wang et al., 2017)

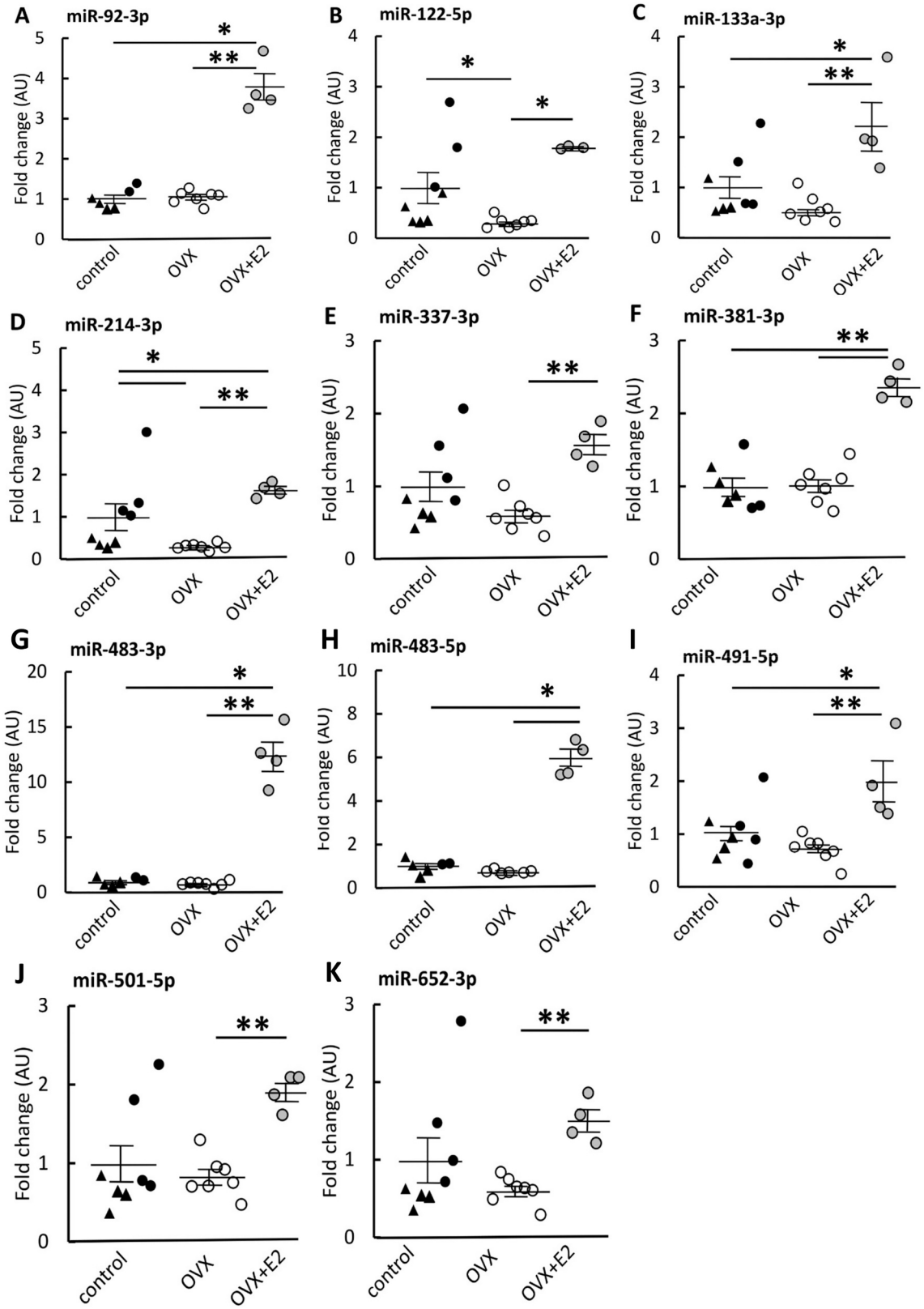

Fig. 2. miR expression in skeletal muscle measured by qPCR. OVX mice had lower expressions of all of the studied miRs compared with OVX + E_2 group (A-K). OVX mice had also lower miR-122-5p and miR-214-3p expression compared with control (B, D). Compared with control, OVX + E_2 group had higher expression of miRs 92a-3p, 133a-3p, 214-3p, −381, 483-3p, 483-5p and 491-5p (A, C, D, F, G, H, I). The control group is comprised of ovary-intact mice with triangles representing mice that did not undergo any surgery and black dots representing sham-operated mice. Results are expressed as mean ± SEM. *$p < 0.050$, **$p < 0.010$.

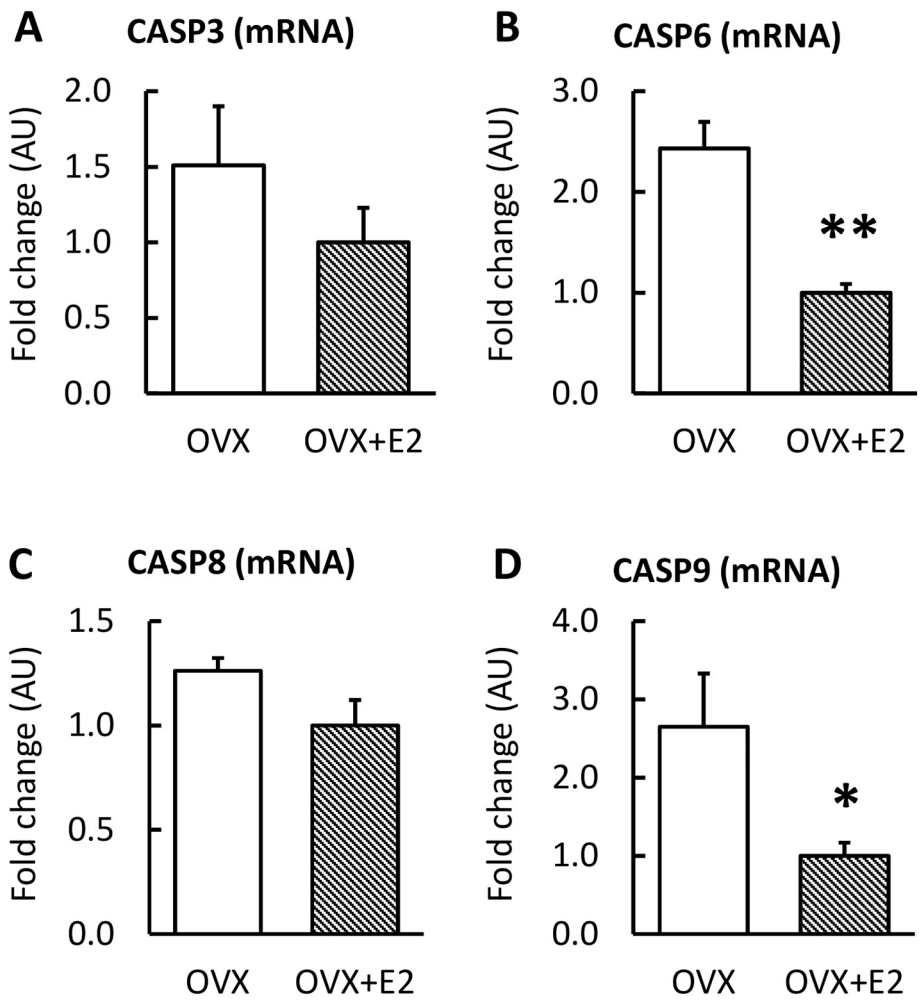

Fig. 3. mRNA expression of caspases 3, 6, 8 and 9 in skeletal muscle measured by qPCR. OVX mice had higher expression of CASP6 and CASP9 compared with OVX + E_2 (B, D). Results are expressed as mean + SEM. *p < 0.050, **p < 0.010.

the initiation of skeletal muscle apoptosis through miRs coordinating the intrinsic apoptotic pathway although downregulation of miRs was also measured contributing to a concomitant upregulation of some of anti-apoptotic agents. Our data suggests that E_2 deficiency may play a role in the initiation of skeletal muscle apoptosis through miRs coordinating the intrinsic apoptotic pathway.

4.1. Estradiol deficiency in skeletal muscle is associated with decreased expression of several miRs linked to apoptosis

We found that the eleven apoptosis-linked miRs, miR 92a-3p, 122-5p, 133a-3p, 214-3p, 337-3p, 381-3p, 483-3p, 483-5p, 491-5p, 501-5p and 652-3p were less abundant in mice with E_2 deficiency (OVX) compared to those mice treated with E_2 (OVX + E_2) (Fig. 2). The miRs investigated in this study participate in posttranscriptional regulation of several key proteins in apoptosis and highlight the intrinsic apoptotic pathway (Su et al., 2015b).

Previously, transfecting cells with miR-92a-3p mimic decreased cell apoptosis via BCL2 and CASP3 pathways, suggesting an anti-apoptotic role in cell homeostasis (Li et al., 2019). In our results E_2 deficiency was associated with low miR-92a-3p level in muscle. In turn, miR-122 upregulation has been shown to induce apoptosis in cardiomyocytes and liver cells (Wu et al., 2009; Zhang and Jing, 2018). Supporting this observation, miR-122 inhibition led to increased expression of anti-apoptotic protein BCL-XL together with lower expression of pro-apoptotic CASP3 (Zhang and Jing, 2018). Similarly, upregulation of miR-133a induced apoptosis in osteosarcoma cell lines, whereas its downregulation strongly correlated with tumor progression (Ji et al., 2013). Furthermore, restoring miR-133a/b has been proposed to be a key therapeutic target for gastric cancer treatment in humans (Liu et al., 2015). It seems that miR-133a acts as a tumor-suppressor in cancer cells by targeting BCL-XL and CASP9 (Liu et al., 2015; He et al., 2011). Similarly, with miRs 122-5p and 133a-3p, upregulation of miR-214-3p is associated with downregulation of BCL-W and vice versa, suggesting a pro-apoptotic role of miR-214-3p (Fan and Wu, 2017). In our study, E_2 deficiency led to low levels of miRs 122-5p, 133a-3p and 214-3p in muscle, which according to previous literature could lead to decreased apoptosis (e.g., [45, 47, 61,]). However, the high levels of these miRs in OVX + E_2 mice was not associated with low levels of their anti-apoptotic target proteins BCL-2 or BCL-XL or a higher CASP8 level (Table 3), but lower p53 transcript and higher BCL-W protein levels. These results indicate that these miRs may share an anti-apoptotic role in skeletal muscle.

Cell experiments with miR-337-3p have yield contradicting results. Experiments with PANC-1 cells show that overexpression of miR-337-3p downregulates CASPs 3 and 7 (Park et al., 2018) yet ectopic expression of miR-337 malignant T cells resulted in increased CASP3 and 7 activity while decreasing BCL2 expression and increasing apoptosis (Xia et al., 2019). miR-381-3p shares similar story: studies show that miR-381-3p acts as an oncogenic miRNA that counteracts apoptotic signaling pathways in renal cancer cells (Zhao et al., 2020). However, in different cancer cell lines miR-381 mimics have found to increase CASP3 and

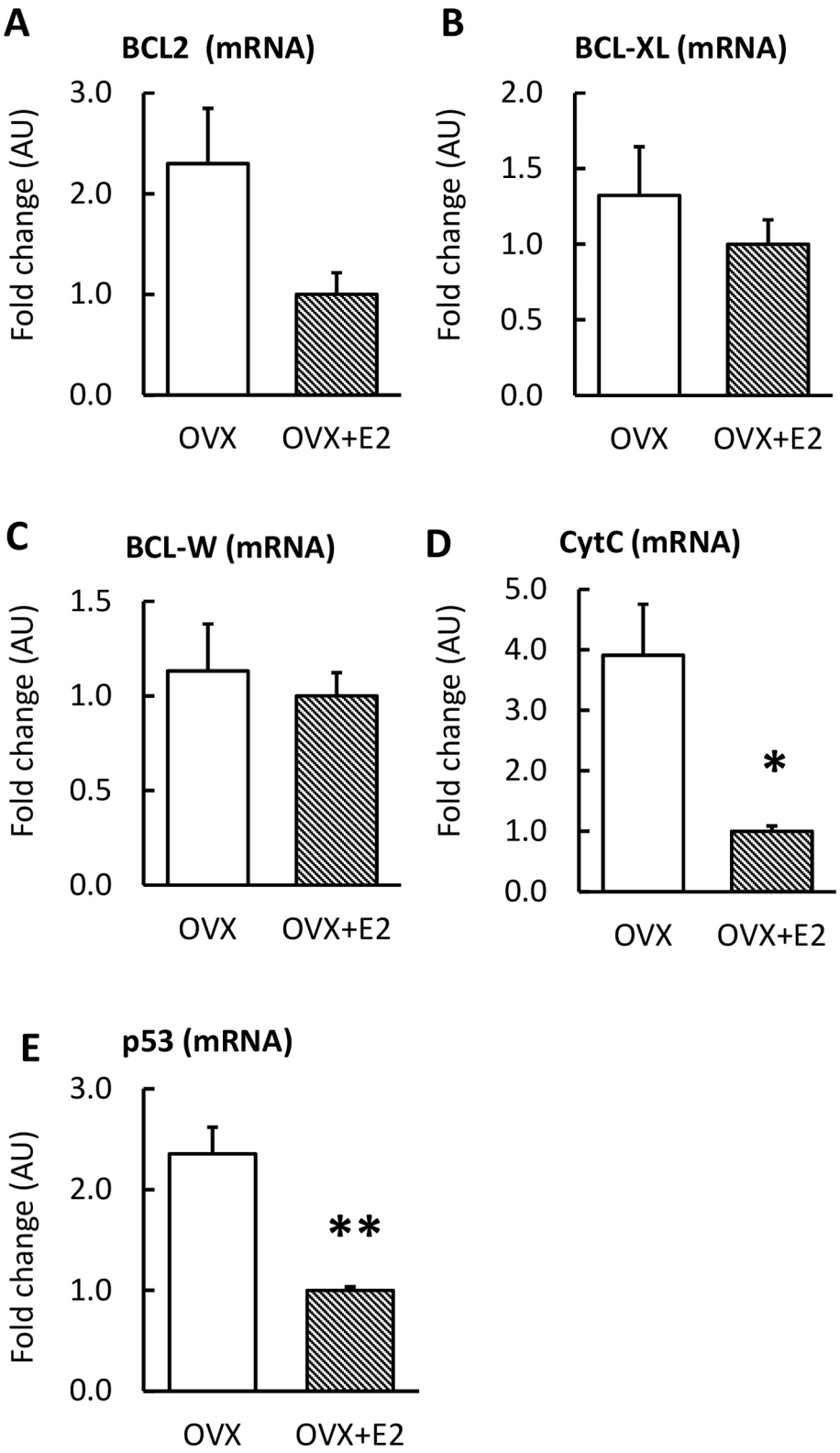

Fig. 4. mRNA expression of BCL2, BCL-XL, BCL-W, cytC and p53 in skeletal muscle measured by qPCR. OVX mice had higher expression of cytC and p53 compared with OVX + E_2 (D, E). Results are expressed as mean + SEM. *$p < 0.050$, **$p < 0.010$.

CASP9 and decrease BCL2 levels whereas its inhibitors have opposing effect (Qiao et al., 2019; Shang et al., 2019). It seems that miR function is sensitive to the cell line used. In our study, E2 deficiency lead to low level of miR337-3p and 381-3p together with higher protein level of active CASP9 in muscle, supporting the anti-apoptotic function of these miRs.

miR-483-3p inhibits apoptosis in breast cancer as well as in renal malignancy tumor cells by regulating SOX3, BAX and BCL2 expressions (Che et al., 2019; Cui et al., 2019). miR-483-5p in turn upregulates CASP3 protein in a kidney cell line (Liu et al., 2019) whereas miR-483-

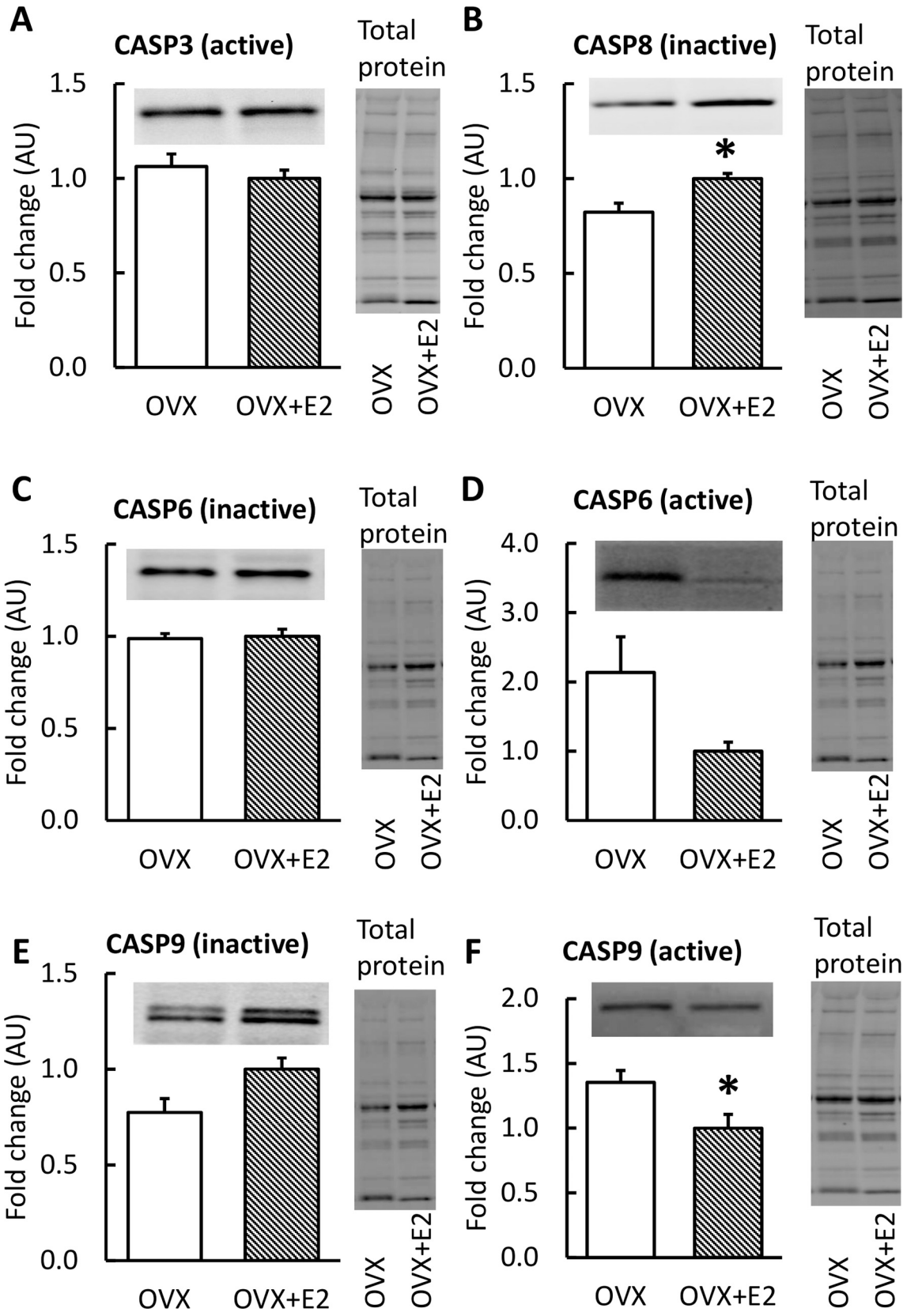

Fig. 5. Protein levels of caspases in skeletal muscle measured by Western Blot with representative blot and total protein images. OVX mice had a lower level of CASP8 (inactive) and higher CASP9 (active) compared with OVX + E_2 (B, F). Results are expressed as mean + SEM. *p < 0.050, **p < 0.010.

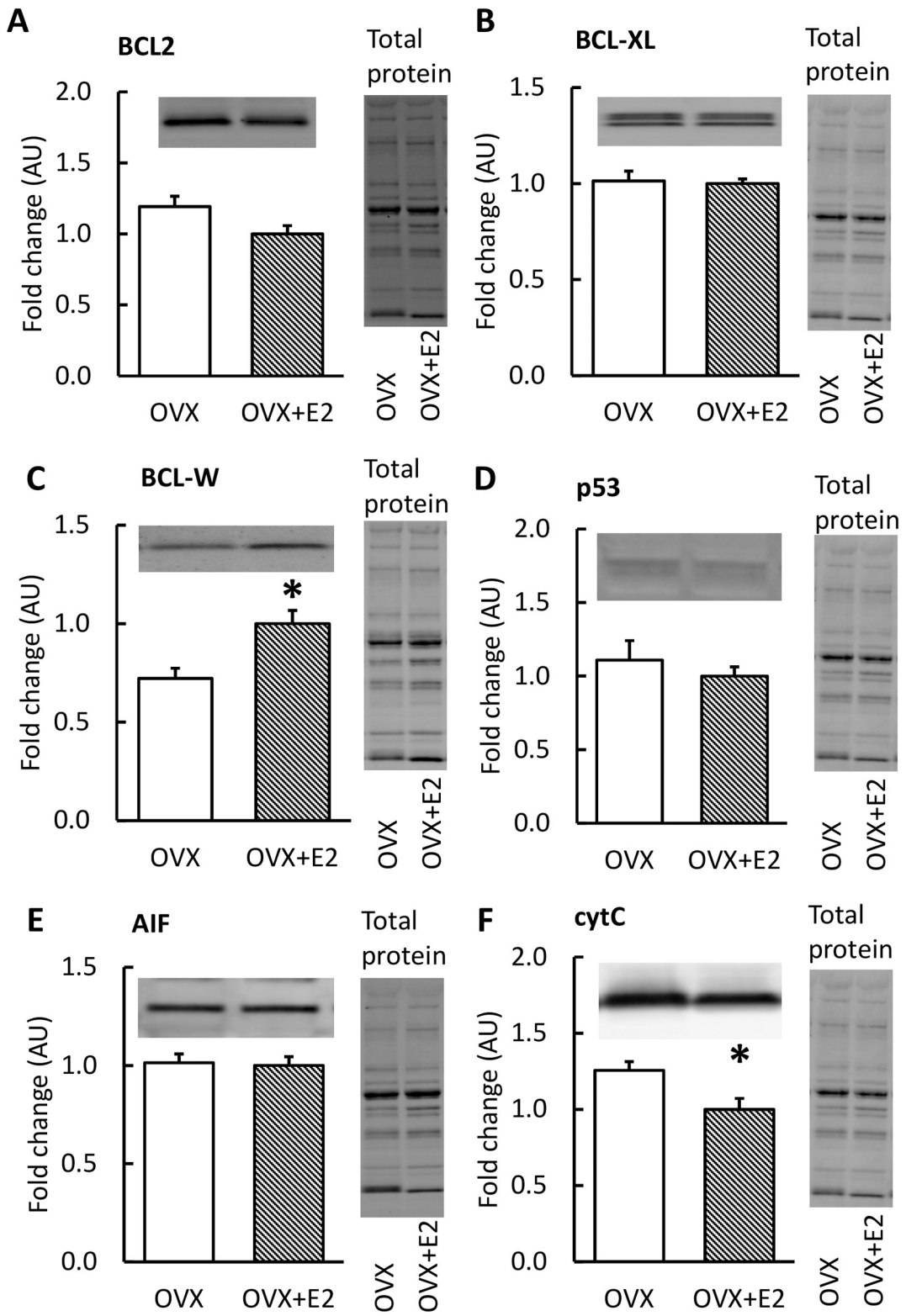

Fig. 6. Protein levels of apoptosis-linked proteins in skeletal muscle measured by Western Blot with representative blot and total protein images. OVX mice had higher levels of BCL-W and cytC compared with OVX + E_2 (C, F). Results are expressed as mean + SEM. *p < 0.050, **p < 0.010.

5p overexpression in gastric cancer cells causes significant upregulation of BCL2 protein (Wu et al., 2016). In contrast, miR-491 induces apoptosis through BCL-XL in human colorectal cancer cells, having therapeutic potential for treating colorectal cancer (Nakano et al., 2010). Experiments with cervical cancer (HeLa) cells shows that miR-501 increase BCL2 expression promoting cervical cancer by inhibited apoptosis (Sanches et al., 2018). In lung cancer cells miR-652 mimic decreased BCL2 and increased the level of CASP3, whereas miR-652 inhibitor induced the opposite changes addressing the pro-apoptotic functions of miR-652 (Wang et al., 2017). Our findings showed lower expression levels of miR 483-3p, 483-5p and 501-5p to be associated with E_2 deficiency, which according to previous literature would

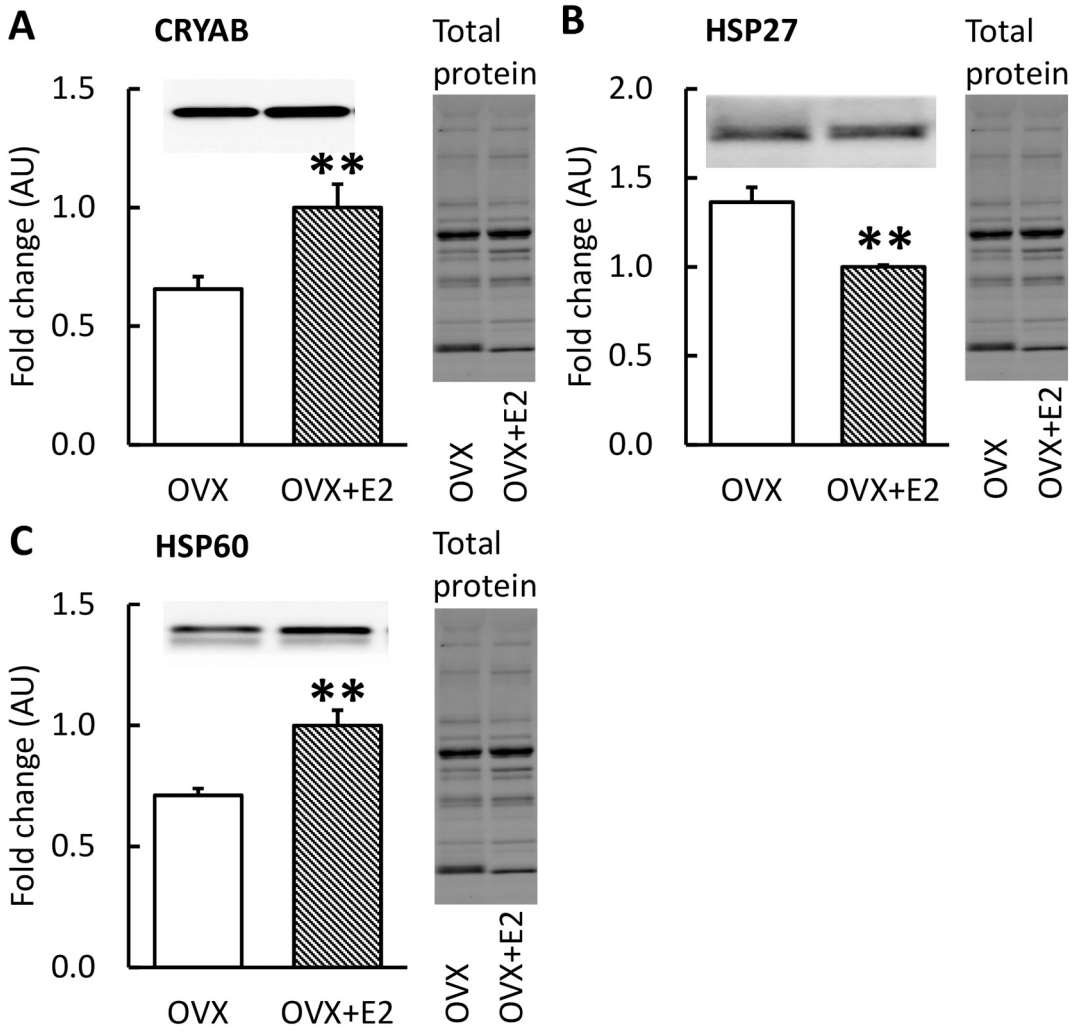

Fig. 7. Protein expression of HSPs in skeletal muscle measured by Western Blot with representative blot and total protein images. OVX mice had lower levels of CRYAB and HSP60 and a higher level of HSP27 compared with OVX + E_2 (A, C). Results are expressed as mean + SEM. *p < 0.050, **p < 0.010.

promote apoptosis. Yet low expression of miR 491-5p and 652-3p were also associated with E_2 deficiency, indicating lower apoptosis.

Our data uniquely shows that miRs that regulate apoptosis in tumor growth in other tissues and cell lines may also coordinate skeletal muscle homeostasis. However, to confirm the direction of the signaling in skeletal muscle (pro- vs. anti-apoptotic) additional comprehensive analysis of the apoptosis signaling pathways together with confirmation of skeletal muscle apoptosis are warranted in the future. Another challenge to consider is that some miRs may regulate both pro- and anti-apoptotic targets (Table 3). According to our results, however, down-regulation of the miRs studied here was largely associated with proapoptosis in skeletal muscle tissue.

4.2. Estradiol deficiency is associated with higher expression of mRNA and apoptosis-linked proteins in skeletal muscle

Several proteins in the intrinsic apoptotic pathway had increased mRNA expression in gastrocnemius muscle from mice in an E_2 deficient state. CASPs 6 and 9 were two of these target proteins (Fig. 3). CASPs are a family of endoproteases whose overexpression and/or increased activity promotes apoptosis (McIlwain et al., 2015). Active CASP6 has shown activity in the cytC-induced apoptosis pathway and is one activator of CASP8 (Cowling and Downward, 2002). Downstream, both intrinsic and extrinsic apoptotic pathways are interconnected via CASP9. Similar to the mRNA results, our data revealed that E_2 deficiency was associated with higher abundance of active CASP9 as well as greater cytC protein levels indicating that the intrinsic apoptotic signaling route has been activated in skeletal muscle of E_2 deficient mice. Furthermore, E_2 deficiency was associated with lower anti-apoptotic BCL-W protein. Consistent with our results, Chung et al. found that in male rats, skeletal muscle ageing led to increased cleaved CASP9, although the level of cleaved CASP3 remained unchanged (Chung and Ng, 2006).

Our previous study showed that serum concentration of FasL was lower in postmenopausal women using hormone replacement therapy compared with non-users, yet did not reveal corresponding differential expression of FasL in muscle (Kangas et al., 2014). FasL belongs to the TNF family and its main function is the induction of extrinsic apoptotic pathway through CASPs 8 and 10 (Hassan et al., 2014; Locksley et al., 2001; Justice et al., 2019). In our present study, replacement of E_2 in ovariectomized mice was associated with increased CASP8 protein in muscle (Fig. 5B) suggesting that E_2 may activate the extrinsic apoptotic pathway. Mechanistically this result is contradicting, as high levels of miRs targeting CASP8 should lead to lower levels of CASP8 mRNA and ultimately protein. However, cell experiments have revealed that miR function may not be as straightforward. In cardiomyocytes overexpression of miR-122 mimic is associated with increased CASP8 expression both at mRNA and protein levels and induced apoptosis (Zhang et al., 2017) consistent with our findings. As miRs may regulate several genes on a specific signaling cascade, it is challenging to predict the ultimate effect of a single miR. Furthermore,the protein measured

here only included the inactive form of CASP8, and it might not correlate with the active form of the protein, as in the case of CASP9 in the present study (Fig. 5E, F). Unfortunately, we were not successful in assaying for active CASP8 protein.

The BCL2-family of proteins act as anti-apoptotic proteins by inhibiting the release of cytC to the cytosol, which in turn activates CASPs. p53 in turn is known to be a pro-apoptotic regulator, which inhibits the activity of BCL2-family members (Hemann, 2006). In our study the only difference in BCL2-proteins was lower BCL-W protein expression in E_2 deficient mice (Fig. 6C) while higher expression of p53 (mRNA level only, Fig. 4E) and higher expression of cytC (both the mRNA and protein levels, Figs. 4D, 6F) were observed in muscle from E_2 deficient mice. In rat skeletal muscle, ageing was associated with higher p53, BCL2 whereas cytC and AIF levels remained unchanged (Chung and Ng, 2006). It seems that E_2 deficiency results in some, yet not all apoptosis-related changes similar to the ageing process.

Previous studies have found a link between estrogen and HSP expression in skeletal muscle (Lee et al., 2007; Vasconsuelo et al., 2010). These studies indicate that estrogen may protect skeletal muscle tissue against apoptosis through HSPs. HSP20-protein family, of which we studied CRYAB and HSP27, consists of the small heat shock proteins, that act as molecular chaperones by preventing misfolding of proteins (Benjamin and McMillan, 1998). In addition, small HSPs inhibit apoptosis by binding and inhibiting CASP function (Kamradt et al., 2001). Similar to small HSPs, HSP60 participates to maintain protein homeostasis and correct folding (Marino Gammazza et al., 2018; Kirchhoff et al., 2002). Ageing results in increased HSP27 and HSP60 in rat skeletal muscle (Chung and Ng, 2006) whereas the effect of estrogen status on HSP27 is still unclear (Collins et al., 2019b). In our study E_2 deficiency was associated with lower levels of CRYAB and HSP60 (Fig. 7). Hence, our data indicates that E_2 deficiency is associated with lower capacity of the muscle tissue to fight against misfolded proteins. However, HSP27 did not follow the trends of the two other HSPs studied here having higher expression in E_2-deficient mice (Fig. 7). Studies done in C2C12 cell line have shown that estrogen treatment protects the cells against apoptosis induced by hydrogen peroxide through upregulation of HSP27 (Vasconsuelo et al., 2010). It seems that HSP27 responds to estrogen in cell injury-related apoptosis signaling, yet the response is not the same when E_2 is diminished systemically.

4.3. Study strengths and limitations

This study investigated apoptosis signaling networks at miR, mRNA and protein levels including key steps in the apoptosis signaling cascade. In the apoptosis variables measured, our study groups of gastrocnemius muscles from female mice with estrogen manipulations represented very modest standard error of means, indicating that our study groups were homogenous and represented well the phenotype desired. In the OVX mice, vaginal cytology confirmed successful ovariectomy and in addition, mice in OVX group were heavier than mice in OVX + E_2 group, which is natural and demonstrated in several publications (see for example (Moran et al., 2007; Rogers et al., 2009)). One limitation of our study is that estrous cycle was not controlled for at the sacrification of the control mice. To avoid possible confounding effect of the cyclic nature of systemic E_2 level in our results, we investigated expression levels of miR-targets by focusing on the mice groups of the lowest systemic E_2 level (OVX) and the constantly high E_2 level (OVX + E_2). It would have been ideal to measure serum E_2 to confirm physiological levels in the OVX + E_2 mice but reproducible, sensitive measurements were not available at the time of this study. We are confident that levels were in the physiological range because we have used the exact same pellets in previous studies (e.g., (Moran et al., 2007)) and in a study subsequent to this study (Le et al., 2018). Another limitation is that we did not have muscle samples available for TUNEL staining which would have been useful in estimating the rate of apoptosis. Recently, we reported that 8 weeks of E_2 deficiency resulted in nearly 4-fold more apoptotic cells in tibialis anterior muscles of ovariectomized mice than controls and E_2 treatment to OVX mice protected cells from apoptosis (Collins et al., 2019a). In that study as in the current study, we did not expect to observe muscle fiber loss nor loss of muscle mass as the duration of the experiments were limited. Here we report the beginning of the apoptosis signaling cascades that are activated in response to estradiol deficiency, which in the long term may affect muscle mass and function.

5. Conclusions

In skeletal muscle from E_2 deficient mice, several apoptosis-linked miRs were downregulated concomitant with higher mRNA expression of the target proteins. Furthermore, E_2 deficiency was associated with lower anti-apoptotic BCL-W and higher pro-apoptotic cytC and active CASP9 protein levels. To conclude, E_2 deficiency downregulated several miRs related to apoptotic pathways that may represent a mechanism that results in increased apoptosis and reduced skeletal muscle mass in estrogen-deficient females including postmenopausal women.

Supplementary data to this article can be found online at https://doi.org/10.1016/j.exger.2021.111267.

Ethics statement

The study protocol was approved by the Institutional Animal Care and Use Committee at the University of Minnesota, USA, which operates under the national guidelines set by the Association for Assessment and Accreditation of Laboratory Animal Care.

Consent for publication

Not applicable.

Availability of data and materials

All data generated or analyzed during this study are included in this published article.

Funding

This project was funded by the Academy of Finland (grants 309504, 314181 and 335249 to EKL) and NIH grants R01 AG031743 and R01 AG062899 (to DAL). GL was supported by T32 AR050938, CAC by T32 AR007612, and TLM by T32 AG029796.

CRediT authorship contribution statement

DAL and EKL planned the study and analysis. SK ran the qPCR and WB analysis, did the in silico analysis, analyzed the NGS, qPCR and WB data and drafted the manuscript. H-KJ ran the NGS analysis. GL ran the qPCR for the miR targets, CAC and TLM performed surgeries and harvested muscle samples. All authors contributed to the revision of the manuscript and approved the final version of the manuscript.

Declaration of competing interest

The authors declare that they have no competing interests.

Acknowledgements

We thank the laboratory personnel of the Faculty of Sport and Health Sciences for all their help during the project.

References

Bai, S., Nasser, M.W., Wang, B., Hsu, S.H., Datta, J., Kutay, H., et al., 2009. MicroRNA-122 inhibits tumorigenic properties of hepatocellular carcinoma cells and sensitizes these cells to sorafenib. J. Biol. Chem. 284 (46), 32015–32027. November 13.

Bai, T., Liang, R., Zhu, R., Wang, W., Zhou, L., Sun, Y., 2020. MicroRNA-214-3p enhances erastin-induced ferroptosis by targeting ATF4 in hepatoma cells. J. Cell. Physiol. 235 (7–8), 5637–5648. July 01.

Benjamin, I.J., McMillan, D.R., 1998. Stress (heat shock) proteins: molecular chaperones in cardiovascular biology and disease. Circ. Res. 83 (2), 117–132. July 27.

Bondarev, D., Finni, T., Kokko, K., Kujala, U.M., Aukee, P., Kovanen, V., et al., 2020. Physical performance during the menopausal transition and the role of physical activity. J. Gerontol. A Biol. Sci. Med. Sci. 24. November.

Brown, M., Ross, T.P., Holloszy, J.O., 1992. Effects of ageing and exercise on soleus and extensor digitorum longus muscles of female rats. Mech. Ageing Dev. 63 (1), 69–77. March 15.

Che, G., Gao, H., Tian, J., Hu, Q., Xie, H., Zhang, Y., 2020. MicroRNA-483-3p promotes proliferation, migration, and invasion and induces chemoresistance of Wilms' tumor cells. Pediatr. Dev. Pathol. 23 (2), 144–151, 1093526619873491.

Chen, Y., Sun, P., Bai, W., Gao, A., 2016. MiR-133a regarded as a potential biomarker for benzene toxicity through targeting Caspase-9 to inhibit apoptosis induced by benzene metabolite (1,4-benzoquinone). Sci. Total Environ. 571, 883–891. November 15.

Chung, L., Ng, Y.C., 2006. Age-related alterations in expression of apoptosis regulatory proteins and heat shock proteins in rat skeletal muscle. Biochim. Biophys. Acta 1762 (1), 103–109. January 01.

Collins, B.C., Arpke, R.W., Larson, A.A., Baumann, C.W., Xie, N., Cabelka, C.A., et al., 2019a. Estrogen regulates the satellite cell compartment in females. Cell Rep. 28 (2). July 09. (368,381.e6).

Collins, B.C., Laakkonen, E.K., Lowe, D.A., 2019b. Aging of the musculoskeletal system: how the loss of estrogen impacts muscle strength. Bone 123, 137–144. June 01.

Cowling, V., Downward, J., 2002. Caspase-6 is the direct activator of caspase-8 in the cytochrome c-induced apoptosis pathway: absolute requirement for removal of caspase-6 prodomain. Cell Death Differ. 9 (10), 1046–1056. October 01.

Cui, K., Zhang, H., Wang, G.Z., 2019. MiR-483 suppresses cell proliferation and promotes cell apoptosis by targeting SOX3 in breast cancer. Eur. Rev. Med. Pharmacol. Sci. 23 (5), 2069–2074. March 01.

Dar, A.A., Majid, S., Rittsteuer, C., de Semir, D., Bezrookove, V., Tong, S., et al., 2013. The role of miR-18b in MDM2-p53 pathway signaling and melanoma progression. J. Natl. Cancer Inst. 105 (6), 433–442. March 20.

Dirks, A., Leeuwenburgh, C., 2002. Apoptosis in skeletal muscle with aging. Am J Physiol Regul Integr Comp Physiol 282 (2), R519–R527. February 01.

Doherty, T.J., 2003 October 01. Invited review: aging and sarcopenia. J Appl Physiol (1985) 95 (4), 1717–1727.

Evans, W.J., 1995 November 01. What is sarcopenia? J. Gerontol. A Biol. Sci. Med. Sci. 50A, 5–8.

Fan, Y., Wu, Y., 2017. Tetramethylpyrazine alleviates neural apoptosis in injured spinal cord via the downregulation of miR-214-3p. Biomed. Pharmacother. 94, 827–833. October 01.

Fridman, J.S., Lowe, S.W., 2003. Control of apoptosis by p53. Oncogene 22 (56), 9030–9040. December 08.

Green, D.R., Kroemer, G., 2004. The pathophysiology of mitochondrial cell death. Science 305 (5684), 626–629. July 30.

Greising, S.M., Baltgalvis, K.A., Lowe, D.A., Warren, G.L., 2009. Hormone therapy and skeletal muscle strength: a meta-analysis. J. Gerontol. A Biol. Sci. Med. Sci. 64 (10), 1071–1081. October 01.

Guo, R., Wang, Y., Shi, W.Y., Liu, B., Hou, S.Q., Liu, L., 2012. MicroRNA miR-491-5p targeting both TP53 and Bcl-XL induces cell apoptosis in SW1990 pancreatic cancer cells through mitochondria mediated pathway. Molecules 17 (12), 14733–14747. December 11.

Hassan, M., Watari, H., AbuAlmaaty, A., Ohba, Y., Sakuragi, N., 2014. Apoptosis and molecular targeting therapy in cancer. Biomed. Res. Int. 2014, 150845.

He, B., Xiao, J., Ren, A.J., Zhang, Y.F., Zhang, H., Chen, M., et al., 2011. Role of miR-1 and miR-133a in myocardial ischemic postconditioning. J. Biomed. Sci. 18, 22–0127. March 16.

Hemann, M.T., Lowe, S.W., 2006. The p53-Bcl-2 connection. Cell Death Differ. 13 (8), 1256–1259. August 01.

Hou, Y., Wei, H., Luo, Y., Liu, G., 2010. Modulating expression of brain heat shock proteins by estrogen in ovariectomized mice model of aging. Exp. Gerontol. 45 (5), 323–330. May 01.

Ji, F., Zhang, H., Wang, Y., Li, M., Xu, W., Kang, Y., et al., 2013. MicroRNA-133a, downregulated in osteosarcoma, suppresses proliferation and promotes apoptosis by targeting Bcl-xL and Mcl-1. Bone 56 (1), 220–226. September 01.

Joza, N., Pospisilik, J.A., Hangen, E., Hanada, T., Modjtahedi, N., Penninger, J.M., et al., 2009. AIF: not just an apoptosis-inducing factor. Ann. N. Y. Acad. Sci. 1171, 2–11. August 01.

Juppi, H.K., Sipila, S., Cronin, N.J., Karvinen, S., Karppinen, J.E., Tammelin, T.H., et al., 2020. Role of menopausal transition and physical activity in loss of lean and muscle mass: a follow-up study in middle-aged Finnish women. J. Clin. Med. 9 (5) https://doi.org/10.3390/jcm9051588. May 23.

Justice, J.N., Nambiar, A.M., Tchkonia, T., LeBrasseur, N.K., Pascual, R., Hashmi, S.K., et al., 2019. Senolytics in idiopathic pulmonary fibrosis: results from a first-in-human, open-label, pilot study. EBioMedicine 40, 554–563. February 01.

Kamradt, M.C., Chen, F., Cryns, V.L., 2001. The small heat shock protein alpha B-crystallin negatively regulates cytochrome c- and caspase-8-dependent activation of caspase-3 by inhibiting its autoproteolytic maturation. J. Biol. Chem. 276 (19), 16059–16063. May 11.

Kangas, R., Pollanen, E., Rippo, M.R., Lanzarini, C., Prattichizzo, F., Niskala, P., et al., 2014. Circulating miR-21, miR-146a and Fas ligand respond to postmenopausal estrogen-based hormone replacement therapy—a study with monozygotic twin pairs. Mech. Ageing Dev. 143–144, 1–8. December 15.

Kirchhoff, S.R., Gupta, S., Knowlton, A.A., 2002. Cytosolic heat shock protein 60, apoptosis, and myocardial injury. Circulation 105 (24), 2899–2904. June 18.

Knowlton, A.A., Korzick, D.H., 2014. Estrogen and the female heart. Mol. Cell. Endocrinol. 389 (1–2), 31–39. May 25.

Krol, J., Loedige, I., Filipowicz, W., 2010. The widespread regulation of microRNA biogenesis, function and decay. Nat Rev Genet 11 (9), 597–610. September 01.

La Colla, A., Vasconsuelo, A., Boland, R., 2013. Estradiol exerts antiapoptotic effects in skeletal myoblasts via mitochondrial PTP and MnSOD. J. Endocrinol. 216 (3), 331–341. February 25.

Laakkonen, E.K., Soliymani, R., Karvinen, S., Kaprio, J., Kujala, U.M., Baumann, M., et al., 2017. Estrogenic regulation of skeletal muscle proteome: a study of premenopausal women and postmenopausal MZ cotwins discordant for hormonal therapy. Aging Cell 16 (6), 1276–1287. December 01.

Le, G., Novotny, S.A., Mader, T.L., Greising, S.M., Chan, S.S.K., Kyba, M., et al., 2018. A moderate oestradiol level enhances neutrophil number and activity in muscle after traumatic injury but strength recovery is accelerated. J. Physiol. 596 (19), 4665–4680. October 01.

Lee, C.E., McArdle, A., Griffiths, R.D., 2007. The role of hormones, cytokines and heat shock proteins during age-related muscle loss. Clin. Nutr. 26 (5), 524–534. October 01.

Li, X., Guo, S., Min, L., Guo, Q., 2019. Zhang S. miR-92a-3p promotes the proliferation, migration and invasion of esophageal squamous cell cancer by regulating PTEN. Int. J. Mol. Med. 44 (3), 973–981. September 01.

Liu, Y., Zhang, X., Zhang, Y., Hu, Z., Yang, D., Wang, C., et al., 2015. Identification of miRNomes in human stomach and gastric carcinoma reveals miR-133b/a-3p as therapeutic target for gastric cancer. Cancer Lett. 369 (1), 58–66. December 01.

Liu, K., He, B., Xu, J., Li, Y., Guo, C., Cai, Q., et al., 2019. miR-483-5p targets MKNK1 to suppress Wilms' tumor cell proliferation and apoptosis in vitro and in vivo. Med. Sci. Monit. 25, 1459–1468. February 24.

Locksley, R.M., Killeen, N., Lenardo, M.J., 2001. The TNF and TNF receptor superfamilies: integrating mammalian biology. Cell 104 (4), 487–501. February 23.

Lu, S., Yu, Z., Zhang, X., Sui, L., 2020. MiR-483 targeted SOX3 to suppress glioma cell migration, invasion and promote cell apoptosis. Onco Targets Ther 13, 2153–2161. March 09.

Maltais, M.L., Desroches, J., Dionne, I.J., 2009. Changes in muscle mass and strength after menopause. J. Musculoskelet. Neuronal Interact. 9 (4), 186–197. December 01.

Marino Gammazza, A., Macaluso, F., Di Felice, V., Cappello, F., Barone, R., 2018. Hsp60 in skeletal muscle fiber biogenesis and homeostasis: from physical exercise to skeletal muscle pathology. Cells 7 (12). https://doi.org/10.3390/cells7120224. November 22.

Marzetti, E., Leeuwenburgh, C., 2006. Skeletal muscle apoptosis, sarcopenia and frailty at old age. Exp. Gerontol. 41 (12), 1234–1238. December 01.

McClung, J.M., Davis, J.M., Wilson, M.A., Goldsmith, E.C., Carson, J.A., 2006. Estrogen status and skeletal muscle recovery from disuse atrophy. J Appl Physiol (1985) 100 (6), 2012–2023. June 01.

McIlwain, D.R., Berger, T., Mak, T.W., 2015 April 01. Caspase functions in cell death and disease. Cold Spring Harb. Perspect. Biol. 7 (4) https://doi.org/10.1101/cshperspect.a026716.

Moore, S.E., Voss, J.G., St Pierre Schneider, B., 2019. 17beta-estradiol alters mRNA co-expression after murine muscle injury and mild hypobaria. Exp Biol Med (Maywood) 244 (16), 1454–1462. November 01.

Moran, A.L., Warren, G.L., Lowe, D.A., 2006. Removal of ovarian hormones from mature mice detrimentally affects muscle contractile function and myosin structural distribution. J Appl Physiol (1985) 100 (2), 548–559. February 01.

Moran, A.L., Nelson, S.A., Landisch, R.M., Warren, G.L., Lowe, D.A., 2007. Estradiol replacement reverses ovariectomy-induced muscle contractile and myosin dysfunction in mature female mice. J Appl Physiol (1985) 102 (4), 1387–1393. April 01.

Nakano, H., Miyazawa, T., Kinoshita, K., Yamada, Y., Yoshida, T., 2010. Functional screening identifies a microRNA, miR-491 that induces apoptosis by targeting Bcl-X (L) in colorectal cancer cells. Int. J. Cancer 127 (5), 1072–1080. September 01.

Olivieri, F., Ahtiainen, M., Lazzarini, R., Pollanen, E., Capri, M., Lorenzi, M., et al., 2014. Hormone replacement therapy enhances IGF-1 signaling in skeletal muscle by diminishing miR-182 and miR-223 expressions: a study on postmenopausal monozygotic twin pairs. Aging Cell 13 (5), 850–861. October 01.

Park, J.K., Doseff, A.I., Schmittgen, T.D., 2018. MicroRNAs targeting Caspase-3 and -7 in PANC-1 cells. Int. J. Mol. Sci. 19 (4) https://doi.org/10.3390/ijms19041206. April 16.

Qiao, G., Li, J., Wang, J., Wang, Z., Bian, W., 2019. miR381 functions as a tumor suppressor by targeting ETS1 in pancreatic cancer. Int. J. Mol. Med. 44 (2), 593–607. August 01.

Rogers, N.H., Perfield, J.W., Strissel, K.J., Obin, M.S., Greenberg, A.S., 2009. Reduced energy expenditure and increased inflammation are early events in the development of ovariectomy-induced obesity. Endocrinology 150 (5), 2161–2168. May 01.

Ronkainen, P.H., Kovanen, V., Alen, M., Pollanen, E., Palonen, E.M., Ankarberg-Lindgren, C., et al., 2009. Postmenopausal hormone replacement therapy modifies skeletal muscle composition and function: a study with monozygotic twin pairs. J Appl Physiol (1985) 107 (1), 25–33. July 01.

Ruan, Y., Wu, S., Zhang, L., Chen, G., Lai, W., 2014. Retarding the senescence of human vascular endothelial cells induced by hydrogen peroxide: effects of 17beta-estradiol (E2) mediated mitochondria protection. Biogerontology 15 (4), 367–375. August 01.
Sanches, J.G.P., Xu, Y., Yabasin, I.B., Li, M., Lu, Y., Xiu, X., et al., 2018 April 01. miR-501 is upregulated in cervical cancer and promotes cell proliferation, migration and invasion by targeting CYLD. Chem. Biol. Interact. 285, 85–95.
Sapp, R.M., Shill, D.D., Roth, S.M., Hagberg, J.M., 2017. Circulating microRNAs in acute and chronic exercise: more than mere biomarkers. J Appl Physiol (1985) 122 (3), 702–717. March 01.
Schneider, B.S., Fine, J.P., Nadolski, T., Tiidus, P.M., 2004. The effects of estradiol and progesterone on plantarflexor muscle fatigue in ovariectomized mice. Biol Res Nurs 5 (4), 265–275. April 01.
Shang, A., Zhou, C., Bian, G., Chen, W., Lu, W., Wang, W., et al., 2019 January 01. miR-381-3p restrains cervical cancer progression by downregulating FGF7. J. Cell. Biochem. 120 (1), 778–789.
Sipila, S., Taaffe, D.R., Cheng, S., Puolakka, J., Toivanen, J., Suominen, H., 2001. Effects of hormone replacement therapy and high-impact physical exercise on skeletal muscle in post-menopausal women: a randomized placebo-controlled study. Clin Sci (Lond) 101 (2), 147–157. August 01.
Sitnick, M., Foley, A.M., Brown, M., Spangenburg, E.E., 2006. Ovariectomy prevents the recovery of atrophied gastrocnemius skeletal muscle mass. J Appl Physiol (1985) 100 (1), 286–293. January 01.
Steller, H., 1995. Mechanisms and genes of cellular suicide. Science 267 (5203), 1445–1449. March 10.
Su, Z., Yang, Z., Xu, Y., Chen, Y., Yu, Q., 2015a. MicroRNAs in apoptosis, autophagy and necroptosis. Oncotarget 6 (11), 8474–8490. April 20.
Su, Z., Yang, Z., Xu, Y., Chen, Y., Yu, Q., 2015b. MicroRNAs in apoptosis, autophagy and necroptosis. Oncotarget 6 (11), 8474–8490. April 20.
Sun, R., Liu, Z., Tong, D., Yang, Y., Guo, B., Wang, X., et al., 2017. miR-491-5p, mediated by Foxi1, functions as a tumor suppressor by targeting Wnt3a/beta-catenin signaling in the development of gastric cancer. Cell Death Dis. 8 (3), e2714. March 30.
Taaffe, D.R., Sipila, S., Cheng, S., Puolakka, J., Toivanen, J., Suominen, H., 2005. The effect of hormone replacement therapy and/or exercise on skeletal muscle attenuation in postmenopausal women: a yearlong intervention. Clin. Physiol. Funct. Imaging 25 (5), 297–304. September 01.
Vasconsuelo, A., Milanesi, L., Boland, R., 2010. Participation of HSP27 in the antiapoptotic action of 17beta-estradiol in skeletal muscle cells. Cell Stress Chaperones 15 (2), 183–192. March 01.
Veronese, A., Lupini, L., Consiglio, J., Visone, R., Ferracin, M., Fornari, F., et al., 2010. Oncogenic role of miR-483-3p at the IGF2/483 locus. Cancer Res. 70 (8), 3140–3149. April 15.
Wang, B., Lv, F., Zhao, L., Yang, K., Gao, Y., Du, M., et al., 2017. MicroRNA-652 inhibits proliferation and induces apoptosis of non-small cell lung cancer A 549 cells. Int. J. Clin. Exp. Pathol. 10 (6), 6719–6726.
Wu, C.C., Bratton, S.B., 2013. Regulation of the intrinsic apoptosis pathway by reactive oxygen species. Antioxid. Redox Signal. 19 (6), 546–558. August 20.
Wu, X., Wu, S., Tong, L., Luan, T., Lin, L., Lu, S., et al., 2009. miR-122 affects the viability and apoptosis of hepatocellular carcinoma cells. Scand. J. Gastroenterol. 44 (11), 1332–1339.
Wu, K., Ma, L., Zhu, J., 2016. miR4835p promotes growth, invasion and selfrenewal of gastric cancer stem cells by Wnt/betacatenin signaling. Mol. Med. Rep. 14 (4), 3421–3428. October 01.
Xia, L., Wu, L., Xia, H., Bao, J., Li, Q., Chen, X., et al., 2019. miR-337 suppresses cutaneous T-cell lymphoma via the STAT3 pathway. Cell Cycle 18 (14), 1635–1645. July 01.
Yin, J., Tang, H.F., Xiang, Q., Yu, J., Yang, X.Y., Hu, N., et al., 2011. MiR-122 increases sensitivity of drug-resistant BEL-7402/5-FU cells to 5-fluorouracil via down-regulation of bcl-2 family proteins. Pharmazie 66 (12), 975–981. December 01.
Zhang, X., Jing, W., 2018. Upregulation of miR122 is associated with cardiomyocyte apoptosis in atrial fibrillation. Mol. Med. Rep. 18 (2), 1745–1751. August 01.
Zhang, Z.W., Li, H., Chen, S.S., Li, Y., Cui, Z.Y., Ma, J., 2017 February 06. MicroRNA-122 regulates caspase-8 and promotes the apoptosis of mouse cardiomyocytes. Braz. J. Med. Biol. Res. 50 (2), e5760-431X20165760.
Zhao, C., Zhou, Y., Ran, Q., Yao, Y., Zhang, H., Ju, J., et al., 2020. MicroRNA-381-3p functions as a dual suppressor of apoptosis and necroptosis and promotes proliferation of renal cancer cells. Front Cell Dev Biol 8, 290. April 28.